JVSTA Journal of Vacuum Science & Technology A

Oxidation of gold by ultraviolet light and ozone at 25°C

David E. King

Citation: Journal of Vacuum Science & Technology A **13**, 1247 (1995); doi: 10.1116/1.579869
View online: http://dx.doi.org/10.1116/1.579869
View Table of Contents: http://scitation.aip.org/content/avs/journal/jvsta/13/3?ver=pdfcov
Published by the AVS: Science & Technology of Materials, Interfaces, and Processing

Oxidation of gold by ultraviolet light and ozone at 25 °C

David E. King
National Renewable Energy Laboratory, Golden, Colorado 80401

(Received 26 October 1994; accepted 6 February 1995)

Gold surfaces have been found to be hydrophilic only after exhaustive preparation and with the ultimate care in sample preparation and treatment. The use of a combination of ultraviolet (UV) light and ozone has been described as a viable method of producing a clean, hydrophilic, gold surface. We have found that gold surfaces, which have been either stored in the laboratory after vacuum deposition or purchased as high purity standards, are oxidized by a combination of UV light and ozone generated from a mercury lamp. The samples were characterized with x-ray photoelectron spectroscopy (XPS) and ion scattering spectroscopy (ISS) prior to and after exposure to UV/ozone in a stainless steel box in laboratory air. After the cleaning process gold surfaces were found by XPS to contain less carbon and to be enriched in oxygen. The O 1*s* on the cleaned surface, which was not present on the untreated surface, consisted of two peaks that are attributed to gold oxide and hydroxyl. The oxide layer was found to be 17 ± 4 Å thick by variable angle XPS depth profiling with an initial stoichiometry of Au_2O_3. The oxide was found to be stable to extended exposure to UHV and water and ethanol rinses. ISS compositional depth profiles confirmed the oxide layer thickness and that the hydrated surface layer is removed in the initial sputtering of the oxidized gold. Implications of these results related to the mechanism of self-assembly of thiols on gold are discussed.

I. INTRODUCTION

Gold has long been known to oxidize under the appropriate conditions. The chemisorption of oxygen on Au(111) at 600 °C has been studied by low-energy electron diffraction and found to be stable to above 850 °C.[1] The production of oxidized gold surfaces by dc reactive sputtering, air corona discharge, and rf oxidation has been detailed.[2–4] Gold oxide Au_2O_3 is a well known and commercially available compound.[5–7] Both crystalline and anhydrous gold oxide have been identified and produced in sufficient quantities for the crystal structure and thermodynamic properties to be determined.[8] Amorphous gold oxide, hydrated gold oxide, and hydrated gold hydroxide have been studied extensively on electrode surfaces.[9–12] The correlation of oxide formation on gold single crystals with surface energy on gold electrodes has been examined.[13] The gold oxide generated on gold electrochemically has even been used to study the oxidation of organic materials in fuel cells.[14,15] The surface roughness of gold electrodes can be altered by the nature of the electrochemically grown oxide.[16–20] Gold has been found to reduce carbon dioxide to carbon generating gold oxide, and freshly generated gold surfaces are known to actively chemisorb certain hydrocarbons.[21,22] Interestingly, gold oxide decomposes when heated, yielding metallic gold and ozone.[8]

The purposes of this article are (1) to determine if a definitive relationship exists between oxidized, contaminated (laboratory stored), clean gold surfaces and water contact angles, (2) to elucidate the surface composition of gold surfaces oxidized in UV/ozone, and (3) to hypothesize about why gold surfaces cleaned in UV/ozone are as suitable for self-assembly of thiol-containing molecules as clean gold surfaces.[23–25]

Contact angle measurements have often been used to measure surface energies and determine surface contamination. In general, polar (such as metal oxides) surfaces are hydrophilic with water contact angles of 0°, and nonpolar surfaces are more hydrophilic with water contact angles greater than 0°.[26,27] The surface energy of a clean pure gold surface has been the subject of much debate over the last 60 years and thus the water contact angle has been in dispute both theoretically and experimentally.[28] In 1964 White reported a water contact angle on gold of $60°\pm5°$.[29] Using different techniques to make determinations under a variety of preparation and measurement conditions, other workers reported values ranging from 0° to 65°.[29–34] With surface preparation and cleanliness a major problem in contact angle measurements, Schrader developed a vapor phase transfer ultrahigh vacuum method of determining contact angles in 1968 and extended this work to include the water contact angles on polished gold disks and evaporated gold films.[35,36] Extensive vacuum preparation and cleaning of the gold surfaces yielded water contact angles of 0°. Smith reported the first use of Auger electron spectroscopy to verify the cleanliness of the gold surface prior to contact angle measurement.[37] Vapor deposited gold was analyzed with Auger electron spectroscopy prior to measuring water contact angles at atmospheric pressure under argon. The gold surface was found to have a 0° contact angle which quickly increased to 30°–40° within 10 min of atmospheric exposure. These data suggest that clean gold is hydrophilic, although this may be considered to be the measurement of the water contact angle of argon on gold. In support of Smith's work Gaines found that gold sheets were hydrophilic after a hydrogen flame treatment, but quickly became hydrophobic in room air. No attempt was made to examine the surface of air-exposed, flamed, gold for possible oxidation.[38]

The action of UV light and ozone has been utilized since 1972 as a method of cleaning and oxidizing surfaces and removing organic contamination.[39] Vig has extensively stud-

ied the UV ozone method of cleaning surfaces.[40] He has described a simple apparatus using a low pressure Hg lamp in a closed stainless steel box to effect cleaning of small samples. Vig found that silver, copper, and gold-plated nickel were extensively oxidized upon extended treatment in an ozone box, while stainless steel, gold, and Kovar appeared unchanged. Gold surfaces cleaned with UV/ozone were found to have modified cohesion properties and appear to improve the reliability of wire bonds.[41] The UV ozone cleaning method also has been used to oxidize GaAs surfaces, to clean silicon wafers, to clean and passivate Ge wafers, to reduce defect densities on GaAs wafers, and to clean complex shapes of gold and silica surfaces.[42–49] Using x-ray photoelectron spectroscopy (XPS) McIntyre *et al.* found that successful UV/ozone cleaning of gold surfaces is limited to the first 10 min of cleaning, and is useful for only a few monolayers of hydrocarbon contamination. Extended exposure results in a gold surface contaminated with CH and CO species, ethers, carbonyl, and carboxyl groups.[49]

The need in our laboratory for relatively large numbers of gold films for use as substrates for self-assembly (SA) of thiol-containing molecules to form organized molecular assemblies (OMAs) has resulted in a search for a reliable method for producing clean gold surfaces on laboratory stored gold films.[24] We previously prepared gold substrates by ion etching single crystal silicon substrates in our Leybold-Heraeus LHS-10 surface analytical system, to remove hydrocarbon and oxide layers, and then evaporating 100–200 nm gold *in situ*.[50] This time-consuming process results in the production of a limited number of very clean gold-coated wafer chips for immediate use as OMA substrates. Since these substrates are made without an adhesion layer they are not suitable for storage. Preparation of gold films using a chromium adhesion layer on Si{100} substrates in a large bell jar system provides samples that have a useable storage life of several months. We have found that laboratory stored gold films not subjected to a cleaning step result in poor OMAs.[51] The surface composition and morphology of gold film substrates can have a varied effect on the properties of the OMA. Contaminants can result in poor film quality with defects, pinholes, and related phenomena that compromise our need to have OMAs that are reproducible for metal overlayer studies.[52] A short cleaning treatment in a UV/ozone box results in the reproducible SA of OMAs.[40] The production and storage of many suitable gold OMA substrates with an ozone/UV cleaning step prior to use has greatly expanded our efforts in the study of OMAs. We have found that UV/ozone cleaned gold films are hydrophilic, while freshly evaporated films, as described above, are hydrophobic.[51–53] The conflicting data on the water contact angle of gold surfaces mean that the relationship between water contact angle and the degree of surface cleanliness of gold is not clear.

Freshly evaporated gold films have been found to be free of O and C contamination upon characterization with XPS and ISS after deposition and hydrophobic upon removal from the vacuum system, with typical water contact angles in excess of 60°.[50,51] These films make excellent substrates for OMAs when used immediately after removal from the ultrahigh vacuum (UHV) system. From our observations freshly evaporated high purity gold films are hydrophobic as are laboratory stored gold films.[24,25,49–53] Gold samples exposed to the highly oxidative environment of the UV/ozone box are hydrophilic for extended periods of time after removal from the chamber and yet often show considerable XPS detectable surface contamination.[51] High resolution XPS analysis also reveals two surface oxygen species and high binding energy features in the Au $4f$ spectra that indicate a hydroxyl gold oxide surface is formed by UV/ozone exposure.

II. EXPERIMENT

Gold was deposited on silicon wafers {100} by the resistive thermal evaporation of 200 nm of 99.9% gold on a 10 nm chromium adhesion layer in a diffusion pumped Varian evaporator at a pressure of 5×10^{-6} Torr.[53] The coated wafers were stored in polypropylene Flouroware® wafer holders in the laboratory ambient until used. Sample coupons for exposure and analysis were cleaved from the gold coated silicon wafers, as needed. Gold standards (99.999% from Metron Co.) for ISS depth profiling and variable angle XPS depth profiling were Ar ion bombarded until found to be free of carbon, oxygen, or any other signal, with XPS (i.e., XPS clean) prior to exposure.

Samples were exposed to UV/ozone in a stainless steel box using a low pressure Hg, ozone generating lamp (BHK, Inc., Bomont, CA).[40] Sample to lamp distance was maintained at 1 cm. The box was placed in a laboratory hood at ambient temperature, nominally 25 °C. The temperature of the ozone box was stable with the normal airflow around the box. Contact angles were measured with a Rame–Hart goniometer using deionized water in the laboratory ambient environment.[51,54]

XPS and ISS data were obtained with the LHS-10 surface analysis system. Details of the system configuration have been given previously.[55] Photoelectrons were excited with Mg $K\alpha$ x radiation from a nonmonochromatic dual Mg/Al x-ray anode operating at 240 W, and detected with a hemispherical analyzer. Variable angle XPS analysis was conducted by rotating the sample rod from the normal incidence to effect nondestructive depth profiling of the sample surface. Survey XPS spectra were acquired in the constant transmission mode with a retarding factor of 3, and high resolution spectra were collected at a constant pass energy of 50 eV. The base pressure of the turbomolecularly pumped UHV chamber during XPS analysis was typically 9×10^{-9} Torr or better. Pressure during ISS analysis was maintained at 4×10^{-7} Torr with ^{3}He. ISS depth profiles were acquired at beam current densities of 19 μA cm^{-2} with an incident beam angle of about 30° with a 123° scattering angle. For the analysis of narrow scan XPS peak positions, widths, and areas a nonlinear least-squares, curve-fitting program (Peak Fit®, Jandel Scientific) was employed. The unsmoothed data were fitted with a Gauss–Lorentzian product function.

Atomic force microscopy (AFM) and scanning tunneling microscopy (STM) (Autoprobe LS, Park Scientific Instruments) analysis was done on stored, water and ethanol rinsed

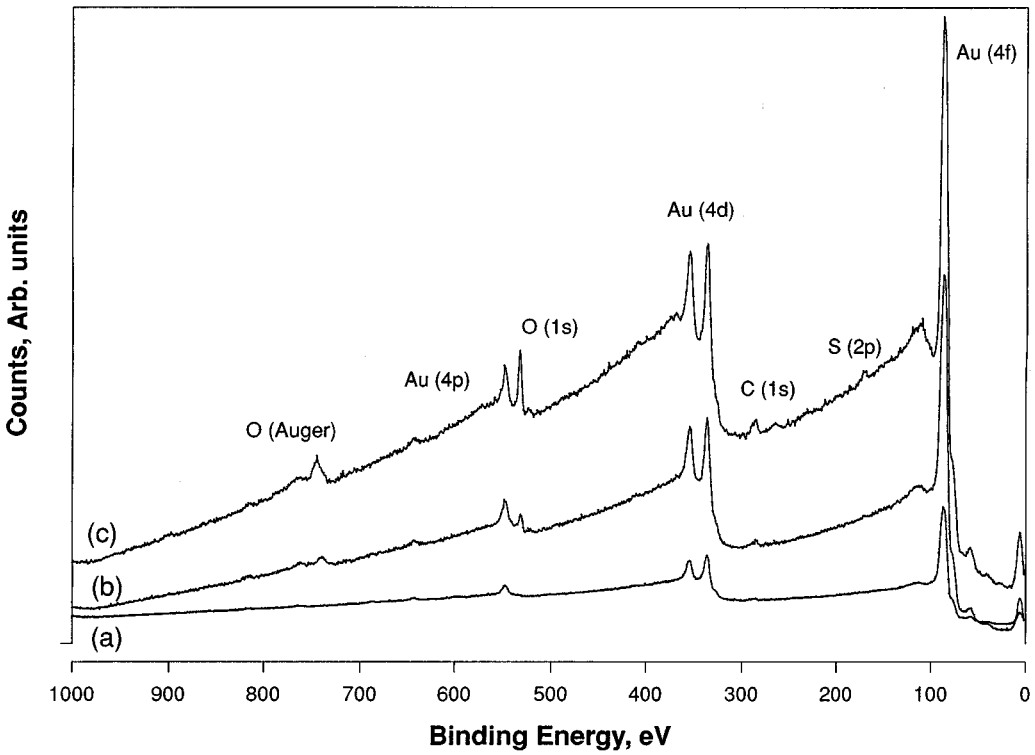

FIG. 1. XPS spectra of clean, ion bombarded gold film (a) compared with gold films exposed to UV/ozone for (b) 1 h and (c) 3 h, respectively. Short exposures to UV/ozone result primarily in oxidation of the gold surface without complete removal of hydrocarbon contamination, and extended exposures result in additional surface contamination and oxidation.

gold films, and on films exposed for a total of 8 h to UV/ozone. The exposed samples were spin rinsed at 1 h intervals with water and ethanol.

III. RESULTS AND DISCUSSION

A. XPS of hydrophobic (and hydrophilic) gold (oxide) surfaces

Samples of freshly evaporated gold films, ion bombarded high purity gold standards, and laboratory stored gold are all hydrophobic with water contact angles in excess of 60°. Following a short 10–15 min exposure to UV/ozone the gold surfaces become hydrophilic. From survey XPS analysis of UV/ozone treated samples we have found that adventitious surface contamination, from storage in the ambient laboratory, was reduced but not eliminated and a substantial increase in the oxygen signal was seen. In Fig. 1 the survey spectrum of a lightly ion bombarded gold standard is compared with the same sample after a 1 h exposure in the UV/ozone box. High resolution XPS spectra of the Au $4f$ region of the UV/ozone exposed sample shows prominent high binding energy (HBE) shoulders on the gold $4f$ photolines indicative of a metal oxide.[3,4,56–58] Curve fitting the high resolution oxygen spectrum yields a two-component peak, consistent with surface hydroxyl and metal oxide.[57,59] An extensive curve-fitted variable angle XPS analysis of these features is provided below. Extended ozone/UV exposure, greater than 1 h, results in some additional surface oxygen; however, other contaminants are also detected. In addition to carbon and oxygen, sulfur (8%), trace nickel (0.4%), and chlorine are seen, [Fig. 1(c)]. The laboratory air is the most likely source of the sulfur, and extended exposure to UV/ozone is known to produce stable surface C and O species.[49] The presence of nickel can be attributed to oxide scale deposited on the sample from the stainless steel ozone box.

Extended XPS analysis of UV/ozone exposed gold samples result in a loss of oxygen signal intensity from exposure to the x-ray flux, and a corresponding loss in the HBE shoulder in the high resolution spectrum of gold. This is consistent with the reduction of gold oxide under x-ray bombardment.[4,57,58] Samples of ozone/UV treated gold also show a loss in oxygen signal after exposure to 12 h vacuum at 10^{-9} Torr. Upon removal from the vacuum chamber the gold surface is hydrophilic, which is consistent with preserving the surface oxide that has been dehydrated in the vacuum chamber. Rinsing the sample with water (rehydrating the gold oxide) and returning it to the UHV system result in some degradation of the instrument vacuum and an increase in the XPS detectable surface oxygen content, Fig. 2.

B. Variable angle XPS data

A gold standard was Ar ion bombarded in the LHS system until XPS clean, exposed in a UV/ozone box for 1 h, and immediately removed to the Leybold UHV surface analysis chamber. Both survey and narrow scan XPS spectra were acquired at three different takeoff angles to effect variable angle (VA) XPS depth profiling. Figure 3 shows curve-fitted Au $4f$ and O $1s$ data, and the specifics of the curve-fitted analysis are given in Tables I–III. The analysis shows two

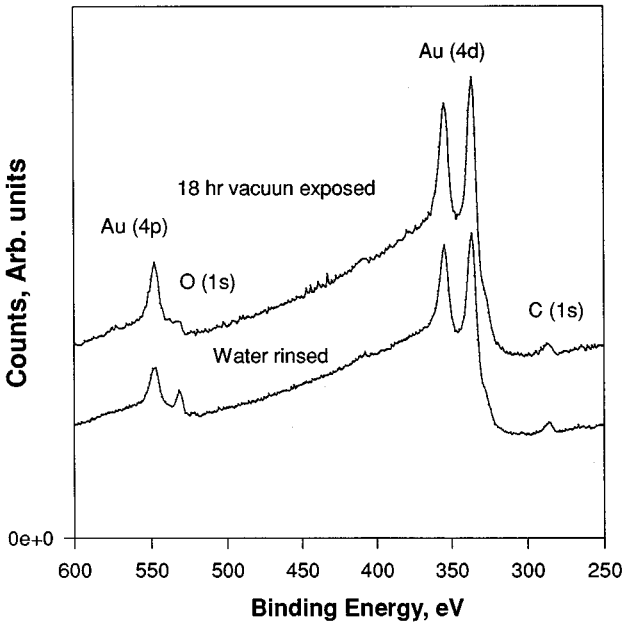

FIG. 2. XPS spectra of a UV/ozone oxidized gold film after 8 h exposure to ultrahigh vacuum, and the same film after a deionized water rinse. The oxide surface is dehydrated in the vacuum chamber but remains stable and is easily rehydrated.

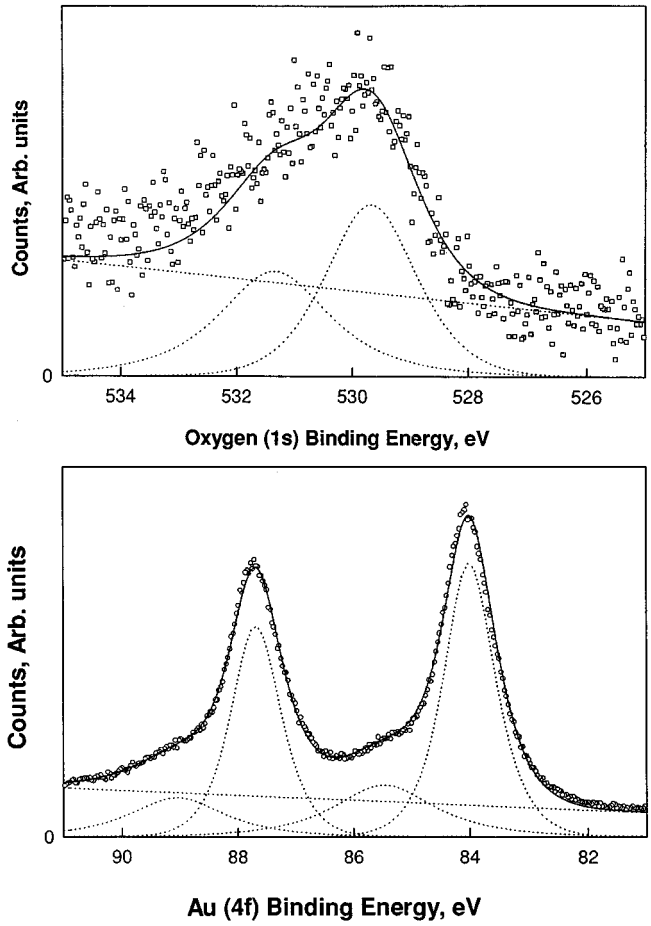

FIG. 3. Curve fitted gold and oxygen XPS spectra taken at 70° takeoff angle from a high-purity gold standard exposed to UV/ozone for 1 h. The two gold peaks shifted to high binding energy from the main $4f$ photolines are representative of gold oxide. The oxygen data were fitted with two peaks representing the oxide at 529.61 and –OH at 531.36 eV.

gold peaks shifted by 1.4 eV to HBE from the two gold $4f$ photolines. Although this value is 0.5 eV lower than for some published values of Au_2O_3 it is still consistent with gold oxide.[3,57,58] The position and full width at half maximum (FWHM) and the ratios of the $\frac{7}{2}$:$\frac{5}{2}$ gold photolines are all in good agreement throughout the analysis (with r^2 fitting values of 0.994 or better), which indicates a consistently good curve fitting. The surface oxide varies from about 39% to 19% as a function of the takeoff angle and x-ray exposure time. The method of Ebel, Eq. (1), was used to analyze the oxide overlayer thickness on the gold substrate,

$$I_0/I_s = R\ \exp[d/(m\ \cos\ \beta)] - 1, \tag{1}$$

where I_0 and I_s are the photoelectron intensities of the overlayer and substrate at a takeoff angle β and R is a function of the atomic weights, densities, and electron mean free paths of the overlayer and the substrate, given by

$$R = [(AW_s/AW_0)(d_0/d_s)(m_0/m_s)], \tag{2}$$

where the mean free path of the oxide was assumed to be twice that of the metal (40 Å), and the literature value of the density of gold oxide is 11 g cm^{-3}.[9,56,60,61]

Using the above relationships and the tabulated values for gold oxide (Au_2O_3) and gold, the overlayer thickness was calculated to be 17±4 Å (Table I).[62] The decrease in the oxide intensity during the variable angle analysis can be attributed to the decomposition of the oxide under the x-ray beam, consistent with published results of x-ray induced reduction of gold oxide.[57,58] This loss in signal due to decomposition of the oxide was anticipated so the most surface sensitive angle was completed first.

The O $1s$ data were fitted with two peaks centered at 529.6 and 531.4 eV, representing gold oxide and either adsorbed water or most likely–OH.[59] The oxygen XPS data are noisier than the gold data so r^2 fitting values of 0.77 to 0.86 were obtained. The curve fittings are remarkably consistent with only slight variations in the binding energies, peak separations, and FWHM. The ratios of the low binding energy (LBE) and HBE O $1s$ peaks are also very reproducible during the VA analysis and fitting. From these data and attributing the LBE O $1s$ peak to the oxygen in gold oxide and the HBE gold $4f$ peak as the gold component of the oxide overlayer the Au/O stoichiometry is given in Table III. The most surface sensitive angle 70°, as well as the least x-ray exposed, yields a stoichiometry of $AuO_{1.5}$ or Au_2O_3. This ratio decreases as a function of the takeoff angle because the gold oxide is continually reduced under extended exposure to the x-ray beam.

C. ISS analysis

An ISS compositional depth profile (CDP) of a typical UV/ozone oxidized gold surface is shown in Fig. 4. The CDP was acquired with a 4 mm×4 mm rastered $^3He^+$ beam at a current density of 185 nA cm^{-2}. Given the molecular weight of gold oxide (441.94), the density (11 g cm^{-3}) and the vari-

TABLE I. Variable angle gold XPS curve-fitting data.

Takeoff angle	Area[a]	FWHM (eV)	E_B (eV)	r^2 of fit	% oxide (7/2)	Oxide thickness
90°				0.994	18.9	13 Å
Au peak 1	18 654.7	1.01	84.00			
2	3 531.2	1.62	85.42			
3	14 284.7	1.02	87.65			
4	2 529.7	1.59	89.05			
80°				0.996	27.5	17 Å
Au peak 1	8 117.5	1.01	84.00			
2	2 236	2.05	85.47			
3	6 186.1	1.02	87.69			
4	1 358.6	1.89	89.05			
70°				0.996	38.9	21 Å
Au peak 1	7 159.5	1.03	84.00			
2	2 783.1	2.03	85.48			
3	5 389.5	1.02	87.69			
4	1 854.5	1.89	89.05			
Mean oxide thickness						17±4 Å
Au[b] (7/2)	6 316.3	1.1	84.05			
(5/2)	4 801.8	1.1	87.42	0.986		
Au[c] (7/2)			84.00			
(5/2)			87.67			

[a]Areas corrected using the LHS sensitivity factors.
[b]Gold standard, ion bombarded clean, 99.999% Au.
[c]References 57, 58, and 68.

able angle XPS determined oxide thickness of 17 Å, a sputter yield of 0.12 atoms/$^3He^+$ ion is calculated.[6,9,56,60,63] An ozone treated gold film is compared with a laboratory stored gold film in Fig. 5. The UV/ozone cleaned sample shows a rapid increase in the gold signal as compared to the laboratory stored sample. The stored sample shows a much slower increase in the gold ISS signal reaching only half the total area of the treated sample after the same sputtering time and conditions. The UV/ozone treatment produces a surface that is apparently easier to sputter clean than the laboratory stored sample. This is presumably because the total surface carbon is decreased and the remaining carbon species are more conducive to removal.

D. AFM/STM data

The examination of gold and oxidized gold electrode surfaces by STM and AFM has been reported in detail.[20,21,64] In general, the surface roughness and morphology are dependent upon the conditions of electrochemical oxidation and reduction of the surface. Gold films exposed to UV/ozone for 1 h followed by rinses in deionized water and ethanol were found to have an rms surface roughness of 30 Å, the same value as control rinsed samples and stored films. This means that the gold oxide is stable to repeated rinses in water and ethanol and that the UV/ozone treatment does not significantly change the surface morphology of the gold surface.

TABLE II. Variable angle oxygen XPS curve-fitting data.

Takeoff angle	Area	Ratio: LBE/HBE[a]	FWHM (eV)	E_B (eV)	Peak separation (eV)	r^2 of fit
90°	420.8	1.26	1.84	529.61	1.75	0.77
	333.75		23.25	531.66		
80°	491.31	1.24	1.84	529.6	1.75	0.76
	397.38		2.22	531.35		
70°	671.9	1.26	1.84	529.67	1.68	0.86
	531.7		2.22	531.35		

[a]LBE peak attributed to metal oxide; HBE peak attributed to water.

TABLE III. Variable angle XPS Au/O relationships.[a]

Takeoff angle	Corrected LBE oxygen (1*s*) area	Corrected HBE gold (4*f*) area	Stoichiometry LBE O(*s*) HBE Au(4*f*)
90°	668	929.3	$AuO_{0.72}$
80°	780	588.4	$AuO_{1.3}$
70°	1066.5	732.4	$AuO_{1.5}$

[a]Corrected areas derived from LHS-10 sensitivity factors for gold and oxygen but uncorrected for escape depths.

IV. CONCLUSIONS

Ion bombarded high purity gold standards, freshly evaporated gold films, and laboratory stored gold films and standards were all found to have water contact angles of greater than 60°. These hydrophobic (low surface energy) surfaces are thus virtually indistinguishable even though there is a large difference in the nature and degree of surface contamination. A hydrophilic surface can be generated by exposing gold, of any degree of surface cleanliness, to UV/ozone.

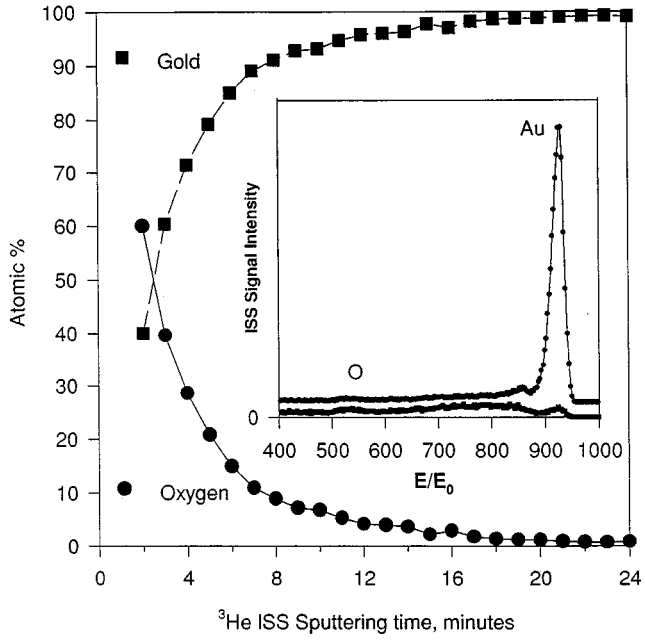

FIG. 4. A ^3He ISS sputter depth profile of a gold film ion bombarded until XPS clean and then exposed for 1 h to UV/ozone. The ISS data were background corrected and the integrated peak areas were converted to atomic percent using surface stoichiometry (Au_2O_3) information from XPS analysis. The inset compares the ISS spectra after 2 and 10 min of ^3He sputtering.

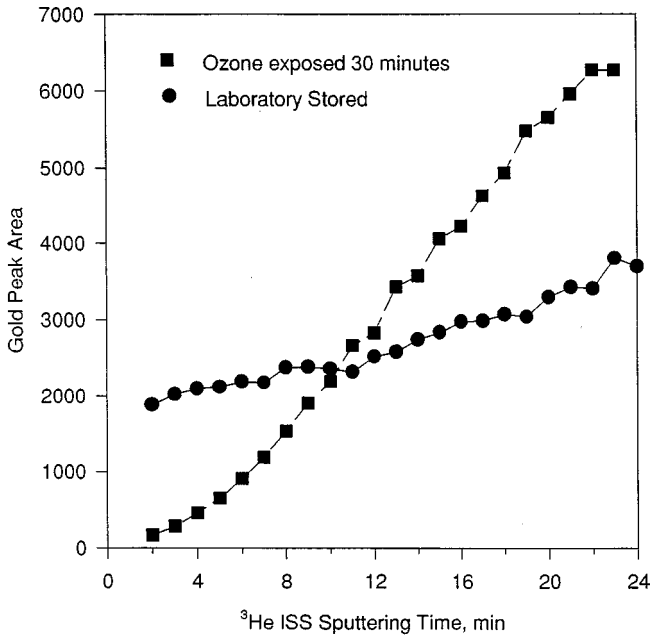

FIG. 5. The integrated gold ISS peak areas from the sputter profiles of laboratory stored and UV/ozone exposed gold films under identical analysis conditions are compared. The gold oxide generated from the UV/ozone exposure is easier to erode to a pure gold surface than contaminants on the laboratory stored gold film. This is most likely due to the hydrocarbons adsorbed on the stored film attenuating the Au ISS signal and reflecting the degree of surface contamination.

Some reduction of surface carbon contamination by the UV/ozone treatment is detected by XPS but the primary surface energy change is due to the formation of gold oxide. Extended exposure to UV/ozone can result in increased surface contamination from ambient air contaminants, such as sulfur, in addition to surface-bound carbon species. For these reasons we conclude that UV/ozone treatment does not produce a clean gold surface and that the contact angle method is not viable for determining the degree of cleanliness of gold surfaces.

From VA XPS depth profiling data we find that XPS clean gold surfaces readily oxidize to a depth of about 17 Å during a 1 h exposure to UV/ozone. The curve-fitted Au $4f$ and O $1s$ XPS data are consistent with a surface stoichiometry of Au_2O_3, and adsorbed –OH. The surface gold oxide was found to be stable to extended vacuum exposure and repeated rinses with water and ethanol. The gold surface morphology also appears unchanged after UV/ozone oxidation and repeated rinses.

ISS depth profiles indicate that an oxidized gold surface is easier to sputter to a single component gold surface than laboratory stored gold surfaces. This may be due to the reduction of the gold under the ion beam, and subsequent rapid loss of surface bound hydrocarbons and oxycarbons. Thus the method of UV/ozone treatment may be a viable method for the surface treatment of gold surfaces for storage of preparation for other cleaning methods, such as sputtering. We would recommend that the UV/ozone treatment be carried out in a quartz tube under a positive pressure of ultra-high purity oxygen in a diluent gas to avoid contamination by atmospheric gases and metal surfaces.[65]

We speculate that the reason thiol molecules successfully self-assemble on UV/ozone treated gold surfaces is that the thiol molecules in solution are oxidized at the Au_2O_3 surface to produce disulfides and a reduced metal surface. This process generates a fresh, metallic, gold surface *in situ* for the self-assembly of thiols and/or the generated disulfides.[22,66,67]

ACKNOWLEDGMENTS

The author would like to thank A. W. Czanderna, J. R. Pitts, and G. Herdt for technical discussions and input, D. Jung for preparing the gold films, and H. Mountinho and the National Renewable Energy Laboratory Nanoscience and Technology Laboratory for the AFM and STM work. This work was performed under DOE Contract No. DE-AC36-83CH10093.

[1]J. Cao, N. Wu, S. Qi, K. Feng, and M. Zei, Chin. Phys. Lett. **6**, 2 (1989).
[2]J. J. Pireaux, M. Liehr, P. A. Thirty, J. P. Delrue, and R. Caudano, Surf. Sci. **141**, 221 (1984).
[3]R. W. Bigelow, App. Surf. Sci. **32**, 122 (1988).
[4]J. M. Baker, J. H. Magerlein, and R. W. Johnson, J. Vac. Sci. Technol. **20**, 175 (1982).
[5]O. Muller, R. E. Newnham, and R. Roy, J. Inorg. Nucl. Chem. **31**, 2966 (1969).
[6]A. Abegg, *Handbook der Anorganischen Chemie* (S. Hirzel, Leipzig, 1908), Vol. 2, p. 819.
[7]W. E. Roseveare and T. F. Buehrer, J. Am. Chem. Soc. **49**, 5 (1927); A. Brunck, Z. Anorg. Chem. **10**, 247 (1895).
[8]P. G. Jones, H. Rumple, E. Schwarzmann, G. Scheldwick, and H. Paulus, Acta. Crystallogr. **35**, 1435 (1979).
[9]M. Sotto, J. Electroanal. Chem. **70**, 1291 (1976).
[10]C. M. Ferro, A. J. Calandra, and A. J. Arvia, Electroanal. Electrochem. **50**, 403 (1974).
[11]C. M. Ferro, A. J. Calandra, and A. J. Arvia, J. Electroanal. Chem. **65**, 963 (1975).
[12]D. T. Sawyer, P. Chooto, and P. S. Tsang, Langmuir **5**, 84 (1989).
[13]R. R. Adzic and S. Strbac, J. Serb. Chem. Soc. **10**, 52 (1987).
[14]R. Celdran, J. Gonzalez-Velasco, and J. Schacho, Abst. XXIX Meeting ISE, Budapest, 1978 (unpublished).
[15]R. Celdran and J. Gonzalez-Velasco, J. Electrochem. Soc. **132**, 10 (1985).
[16]P. A. Thiessen, G. Heinicke, and E. Schober, Z. Anorg. Allg. Chem. **377**, 20 (1970).
[17]D. Dickertmann, J. W. Schultze, and K. J. Vetter, Electro. Anal. Chem. Inter. Electrochem. **55**, 429 (1974).
[18]L. Vazquez, A. Bartolome, A. M. Baro, C. Alonso, R. C. Salvarezza, and A. J. Arvia, Surf. Sci. **215**, 171 (1989).
[19]C. M. Vitus and A. J. Davenport, J. Electrochem. Soc. **141**, 5 (1994).
[20]H. Honbo, S. Sugawara, and K. Itaya, Anal. Chem. **62**, 2424 (1990).
[21]S. Mori and Y. Shitara, Appl. Surf. Sci. **68**, 65 (1993).
[22]M. E. Vela, R. C. Salvarezza, and A. J. Arvia, Electrochem. Acta **35**, 117 (1990).
[23]A. Ulman, *An Introduction to Ultrathin Organic Films* (Academic, New York, 1991).
[24]A. W. Czanderna, D. E. King, and D. Spaulding, J. Vac. Sci. Technol. A **95**, 2607 (1991).
[25]D. R. Jung, D. E. King, and A. W. Czanderna, Appl. Surf. Sci. **70/71**, 127 (1993).
[26]*Symposium on Contact Angle, Wettability and Adhesion*, San Francisco, CA, 1992, edited by K. L. Mittal, American Chemical Society Symposium (VSP, Utrecht, The Netherlands, 1993).
[27]A. Adamson, *Physical Chemistry of Surfaces* (Wiley, New York, 1982).
[28]A. Gorodetzaya and B. Kabanov, Phys. Z. Sowjetunion **5**, 418 (1934).
[29]M. L. White, J. Phys. Chem. **68**, 3083 (1964).
[30]A. C. Zettlemoyer, J. Colloid Interface Sci. **28**, 343 (1968).
[31]M. L. White and J. Drobek, J. Phys. Chem. **70**, 3432 (1966).
[32]R. A. Erb, J. Phys. Chem. **69**, 1306 (1965).

[33]K. W. Bewig and W. A. Zisman, J. Phys. Chem. **69**, 4238 (1965).
[34]R. A. Erb, J. Phys. Chem. **72**, 2412 (1968).
[35]M. E. Schrader, J. Phys. Chem. **74**, 2313 (1970).
[36]M. E. Schrader, J. Colloid. Interface Sci. **27**, 743 (1968).
[37]T. Smith, J. Colloid Interface Sci. **75**, 1 (1980).
[38]G. L. Gaines, J. Colloid Interface Sci. **79**, 3 (1981).
[39]D. A. Bolon and C. O. Kunz, Polm. Eng. Sci. **12**, 109 (1972).
[40]J. R. Vig, J. Vac. Sci. Technol. A **3**, 1027 (1985).
[41]J. L. Jellison, IEEE Trans. Parts. Hybrids Packag. **PHP-11**, 206 (1975).
[42]R. K. Kopf, A. P. Kinsella, and C. W. Ebert, J. Vac. Sci. and Technol. B **9**, 132 (1991).
[43]J. Bennett and J. A. Dagata, J. Vac. Sci. Technol. A **11**, 2597 (1993).
[44]L. Zazzera and J. F. Evans, J. Vac. Sci. Technol. A **11**, 934 (1993).
[45]M. Niwano, K. Kinashi, K. Saito, N. Miyamoto, and K. Honma, J. Electrochem. Soc. **141**, 6 (1994).
[46]X. J. Zhang, G. Xue, A. Agarwal, R. Tsu, M. A. Hasan, J. E. Greene, and A. Rockett, J. Vac. Sci. Technol. A **11**, 2553 (1993).
[47]M. T. Schmidt, D. V. Podlesnik, H. L. Evans, C. F. Yu, E. S. Yang, and R. M. Osgood, J. Vac. Sci. Technol. A **6**, 1446 (1988).
[48]M. Niawano, M. Suemitsu, Y. Ishibashi, Y. Takeda, N. Miyamoto, and K. Honma, J. Vac. Sci. Technol. A **10**, 3171 (1992).
[49]N. S. McIntyre, R. D. Davidson, T. L. Walzak, R. Williston, M. Westcott, and A. Pekarsky, J. Vac. Sci. Technol. A **9**, 1355 (1991).
[50]D. King and A. W. Czanderna, Surf. Sci. Lett. **235**, L329 (1990).
[51]National Renewable Energy Laboratory (unpublished results).
[52]D. R. Jung and A. W. Czanderna, Crit. Rev. Solid State Mater. Sci. **19**, 1 (1994).
[53]D. R. Jung, D. E. King, and A. W. Czanderna, J. Vac. Sci. Technol. A **11**, 2382 (1993).
[54]C. D. Bain, E. B. Troughton, Y. T. Tao, J. Evall, G. M. Whitesides, and R. G. Nuzzo, J. Am. Chem. Soc. **111**, 321 (1989).
[55]J. R. Pitts, T. M. Thomas, and A. W. Czanderna, Appl. Surf. Sci. **26**, 107 (1986).
[56]T. Dickinson, A. F. Povey, and P. Sherwood, J. Chem. Soc. Faraday Trans. **171**, 298 (1975).
[57]J. H. Linn and W. E. Swartz, Appl. Spectrosc. **39**, 755 (1985).
[58]C. R. Aita and N. C. Tran, J. Vac. Sci. Technol. A **9**, 1498 (1991).
[59]J. H. Linn and W. E. Swartz, Appl. Surf. Sci. **20**, 154 (1984).
[60]M. F. Ebel, H. Ebel, and J. Wernich, J. Adv. X-Ray Anal. **23**, 223 (1980).
[61]*Methods of Surface Analysis*, edited by A. W. Czanderna (Elsevier, New York, 1975), pp. 108–109.
[62]*CRC Handbook of Chemistry and Physics*, 74th ed. (Chemical Rubber, Boca Raton, FL, 1994).
[63]L. C. Feldman and J. Mayer, *Fundamentals of Surface and Thin Film Analysis* (North-Holland, Amsterdam, 1986).
[64]J. A. DeRose, D. B. Lampner, S. M. Lindsay, and N. J. Tao, J. Vac. Sci. Technol. A **11**, 776 (1993).
[65]Samco International, manufacturer of UV/ozone cleaning devices.
[66]J. March, *Advanced Organic Chemistry*, 4th ed. (Wiley, New York, 1992).
[67]H. A. Biebuyck and G. M. Whitesides, Langmuir **9**, 1776 (1993).